THE JOURNAL OF PHYSICAL CHEMISTRY B

Article

pubs.acs.org/JPCB

Absorption Band III Kinetics Probe the Picosecond Heme Iron Motion Triggered by Nitric Oxide Binding to Hemoglobin and Myoglobin

Byung-Kuk Yoo,[†] Sergei G. Kruglik,[‡] Isabelle Lamarre,[†] Jean-Louis Martin,[†] and Michel Negrerie*,[†]

[†]Laboratoire d'Optique et Biosciences, INSERM, Ecole Polytechnique, 91128 Palaiseau, France

[‡]Laboratoire Jean Perrin, UPMC Université Paris 06, CNRS FRE 3231, 75005 Paris, France

Supporting Information

ABSTRACT: To study the ultrafast movement of the heme iron induced by nitric oxide (NO) binding to hemoglobin (Hb) and myoglobin (Mb), we probed the picosecond spectral evolution of absorption band III (~760 nm) and vibrational modes (iron–histidine stretching, ν_4 and ν_7 in-plane modes) in time-resolved resonance Raman spectra. The time constants of band III intensity kinetics induced by NO rebinding (25 ps for hemoglobin and 40 ps for myoglobin) are larger than in Soret bands and Q-bands. Band III intensity kinetics is retarded with respect to NO rebinding to Hb and to Mb. Similarly, the $\nu_{(Fe-His)}$ stretching intensity kinetics are retarded with respect to the ν_4 and ν_7 heme modes and to Soret absorption. In contrast, band III spectral shift kinetics do not coincide with band III intensity kinetics but follows Soret kinetics. We concluded that, namely, the band III intensity depends on the heme iron out-of-plane position, as theoretically predicted (Stavrov, S. S. *Biopolymers* **2004**, *74*, 37–40).

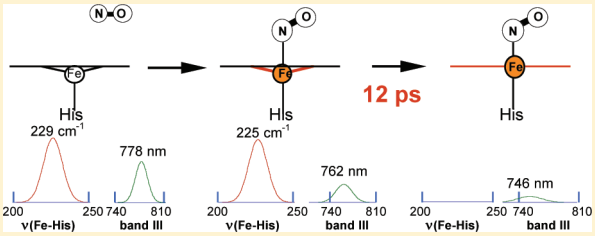

1. INTRODUCTION

The reactivity and activation of heme enzymes which bind a diatomic ligand (O_2, NO, or CO) depend upon the transmission of the binding event to the entire protein structure, which is often multimeric. The binding of diatomics to heme proteins underlines very diverse functions, comprising O_2 transport by hemoglobin (Hb), signal transmission by the endogenous NO receptor guanylate cyclase and response to environment conditions by bacterial CO, NO, and O_2 sensors. The binding and release of these diatomics induce allosteric changes in the protein structure correlated with the activation and deactivation mechanisms, which involve interactions between subunits (for example, in tetrameric Hb and heterodimeric guanylate cyclase). When activation (and/or cooperativity) is induced from a five-coordinate to a six-coordinate iron, the very first triggering event is necessarily the motion of the central heme iron coupled with the motion of the proximal side chain. This motion takes place toward the macrocycle plane when the diatomic ligands O_2 and NO bind to hemoglobin and myoglobin hemes. The hemoglobin crystal structure[1,2] revealed subunit interactions which are underlying in the funding model of allostery,[3] and numerous works were devoted to identify the allosteric structural transitions in different time scales in the Hb tetramer or other heme proteins.[4−12] Structural techniques such as time-resolved resonance Raman (TR^3) and X-ray measurements addressed so far the hemoglobin R → T transition by photodissociation of CO which does not rebind to Hb and Mb in the picosecond–nanosecond time range. In order to probe the opposite process, the primary ultrafast heme response upon diatomic binding, so as to address the T → R transition, we have chosen to study the NO rebinding after photodissociation by a femtosecond laser pulse, used for synchronization of the events.

The out-of-plane iron motion induced by NO or CO dissociation occurs much faster than 1 ps, as measured by transient absorption[13] (TA) and confirmed to be <0.6 ps by Raman spectroscopy[14] and is thus considered quasi-instantaneous when compared to gaseous ligand rebinding kinetics and protein relaxation. However, since the iron motion is coupled to protein backbone dynamics via the bond with proximal side chain, the reverse in-plane iron motion induced by axial ligand binding is not instantaneous, as we have previously discovered from TR^3 spectra.[15] Indeed, the intensity decay of the Fe–histidine stretching following NO rebinding to Mb and various other heme proteins was found to be slower than corresponding TA kinetics which probe the heme coordination state through the Soret visible absorption band (at 420–435 nm, assigned to π–π^* porphyrin transition). We interpreted this observation as the existence of a nonplanar six-coordinate nitrosylated heme, whose lifetime is in the range of 6–40 ps, depending on the protein studied. Our finding was rationalized by previous theoretical calculations[16] explaining how the Fe–His stretching intensity depends upon the position of the iron with respect to the heme plane through heme absorption and resonance. Further theoretical calculations[17,18] focused on the absorption band III of five-coordinate ferrous heme (located in the near-IR at ~760 nm, Figure 1) which is assigned to a transition between the π-porphyrin molecular orbital and d_{yz}

Received: January 26, 2012
Revised: March 5, 2012
Published: March 6, 2012

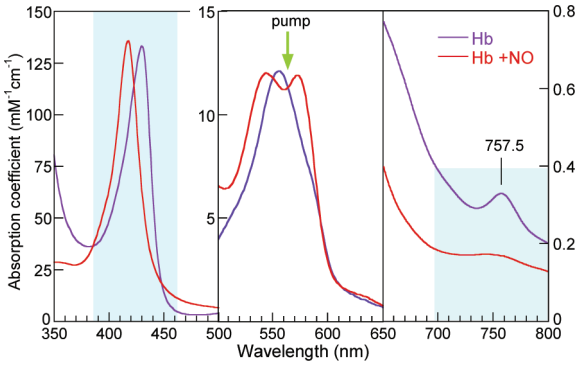

Figure 1. Steady-state absorption spectra of unliganded ferrous hemoglobin (blue curves) and liganded with NO (red curves). The panels disclose successively the Soret absorption band (or γ-band), the Q-bands (or α-, β-bands), and the band III. The colored areas are those probed by time-resolved absorption spectroscopy, and the green arrow indicates the wavelength of the photodissociating pulse.

iron orbital[19,20] (charge-transfer transition). This study[17,18] concluded that the intensity of band III is sensitive to the iron–heme plane distance, as is the central band frequency. The frequency position of band III has been used to probe the relaxation of the five-coordinate heme in Mb[21,22] and dimeric Hb[23] after CO photolysis, a diatomic which does not rebind to Mb in the picosecond time range, while the behavior of band III during geminate rebinding of any gaseous ligand (a fortiori NO) in this time scale is unknown.

In the present study, we measured band III intensity and spectral shift kinetics in the picosecond time range with the aim of probing the primary structural events triggered by NO release and subsequent rebinding in Hb compared to Mb. We compare the kinetics of band III absorption with those originated from the Soret bands and Q-bands and also with the kinetics of iron–histidine stretching, ν_4 and ν_7 vibrational modes intensities from subpicosecond TR^3 spectra.

2. METHODS

2.1. Sample Preparation. Horse heart myoglobin and human hemoglobin A (Sigma-Aldrich) were dissolved in phosphate buffer (pH 7.4). The sample purity was verified by gel electrophoresis. The solution of ferric proteins (100 μL, 50 μM for Soret measurement, 4 mM for band III measurement because the absorption coefficient at 760 nm is only 350 M^{-1}·cm^{-1}) was put in a 1 mm optical path length quartz cell sealed with a rubber stopper and degassed by means of four successive cycles of vacuuming and purging with argon (Air Liquide, 99.999%). Both ferric proteins were reduced by the addition of 10 μL of degassed sodium dithionite ($Na_2S_2O_4$, 10 mM final concentration for band III or 2 mM for Soret measurement). For band III measurement, the ferrous samples yield absorbances of 2.9 (Mb) and 2.1 (Hb) at 564 nm, the wavelength used to photoexcite the sample. Equilibrium spectra were recorded at each step to verify the state of the sample. For preparing NO-liganded proteins, the argon gas phase was replaced by 10% NO gas phase diluted in N_2 (or 1% NO for Soret measurement), directly introduced into the spectroscopic cell still connected to the gas train (at ~1.3 bar) to ensure an "infinite reservoir" of NO during binding equilibration. Because of the larger Mb concentration required for band III measurement, we used a higher NO concentration. However, the kinetics of geminate rebinding in the picosecond–nanosecond time range are not affected because the same photodissociated molecule rebinds and NO molecules do not have time to reach the heme from solvent in this time scale.

For TR^3 measurements, 100 μL of a buffered solution of ferric Hb or Mb at a concentration of 0.3 mM was placed in a cylindrical UV-quartz spinning cell (Hellma, ref 540–135) sealed by a rubber stopper, vacuumed and purged with argon. The absorbance was about 1 in the Q-bands for an optical path length of 1 cm. The reduction of the proteins was performed like for absorption measurements. Then argon was replaced with NO 1%.

2.2. Transient Absorption Spectroscopy. Femtosecond absorption spectroscopy was performed with the pump–probe laser system previously described.[24] The setup provides an excitation pulse at 564 nm (duration 50 fs; repetition rate 30 Hz) for the photodissociation of NO. The amplified pulse at 615 nm (duration 50 fs) produces a pulsed white light continuum after focusing in a 8 mm cell that contained either H_2O (for Soret measurement) or D_2O (for band III measurement) to avoid that spontaneous Raman emission of H_2O (3400 cm^{-1}) overlaps the band III. From this continuum, the probe pulse wavelength is selected by a line of two prisms and a Schott filter for band III (RG-630; 3 mm). Both beams were focused and spatially overlapped in the sample cell, which was continuously moved perpendicularly to the beams for ensuring sample renewal between laser shots. Transient spectra were recorded simultaneously to kinetics by a CCD detector as a time–wavelength matrix of induced absorption. The CCD calibration was performed with a multiline interference filter. The global analysis of the data at Soret band was performed by singular value decomposition (SVD) of this time–wavelength matrix[24] in the time window up to 250 ps. For band III, up to 160 scans were recorded and averaged with a dwell time of 2 s at each point. Band III kinetics were fitted at particular wavelengths and by fitting the time dependence of integrated band III intensity, which was obtained after fitting each individual transient spectrum to the sum of exponential and Gaussian functions. Equilibrium spectra were recorded with a Shimadzu 1700 spectrometer. The accuracy of wavelength determination is ±0.3 nm for steady-state spectra and ±1 nm for transient spectra. All measurements were performed at 20 ± 2 °C. The probed spectral regions are indicated in Figure 1.

2.3. Time-Resolved Resonance Raman Spectroscopy. The time-resolved Raman apparatus has been described in detail elsewhere.[25] Briefly, it has 0.7 ps temporal resolution and 25 cm^{-1} spectral resolution and is based on a femtosecond Ti:Sapphire oscillator and a regenerative laser amplifier (output beam parameters are 810 nm, ~0.6 mJ, 50 fs, 1 kHz), an optical parametric generator, and two optical parametric amplifiers to generate the photodissociating pulse (560–570 nm; 2 μJ; 100 fs) whose delay is controlled and the Raman probe pulse (435 nm; 25 nJ; 0.7 ps; 25 cm^{-1}). Both beams are collinearly superimposed in the cylindrical spinning sample cell. The procedure for obtaining the photoproduct spectra from raw TR^3 spectra was described elsewhere.[25] The photoproduct transient Raman spectra (including the bands ν_{Fe-His}, ν_4, and ν_7) have been fitted to Voigtian contours using Multipeak Fitting package in Igor Pro (WaveMetrics). The details of the relaxation model based on rate equations approach and including the transition from domed to planar six-coordinate heme with time constant τ_D have been previously reported[15] and are presented in extended form in the Supporting

dx.doi.org/10.1021/jp300849y | J. Phys. Chem. B 2012, 116, 4106–4114

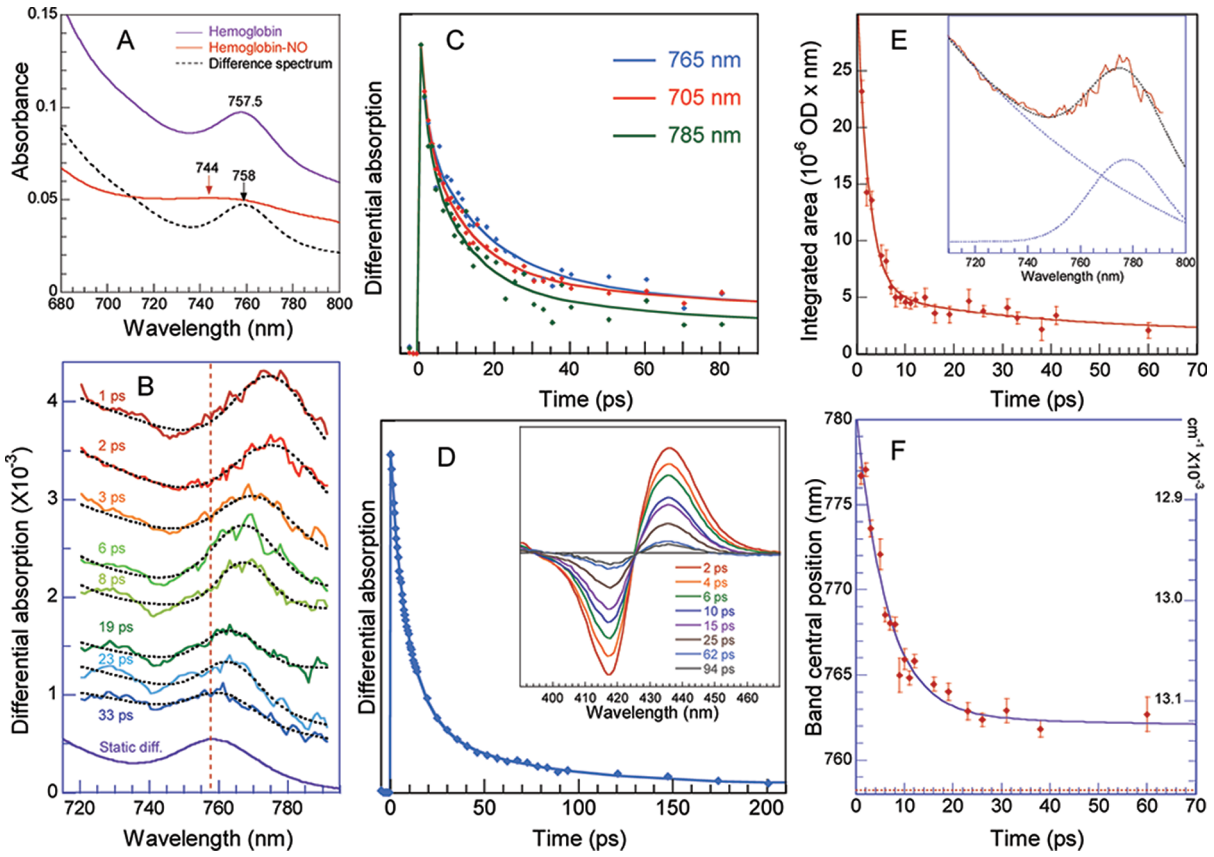

Figure 2. Transient absorption measurement of Hb−NO. (A) Steady-state absorption spectrum in the band III region for Hb and Hb−NO. (B) Transient difference spectra of band III at particular time delays after NO dissociation. The spectrum before dissociation (negative delay) was subtracted from each spectrum at positive delay. The spectra are not offset, and their relative amplitude is that experimentally obtained. For each spectrum, the black dotted line is a fit of the transient band III to a Gaussian function. The red vertical dotted line corresponds to the position of the band III in the steady-state difference spectrum (purple) scaled for comparison. (C) Kinetics at three single wavelengths after Hb−NO photodissociation (fitted parameters in Table 1). (D) Kinetics of NO rebinding to Hb from global analysis of the entire Soret absorption band (fitted parameters in Table 1). Difference transient spectra are disclosed in the inset. (E) Integrated intensity of band III as a function of time. Each individual transient spectrum was fitted to the sum of a Gaussian function (band III) and an exponential function (tail of the Q-band) as detailed in the inset. The area of the Gaussian represents the integrated intensity of band III. This intensity as a function of time was then fitted to a sum of exponential functions (τ_{vib} = 2.4 ± 0.6 ps; τ_1 = 25 ± 6 ps; τ_2 = 120 ± 35 ps). (F) Central position of the fitted Gaussian as a function of time. The kinetics of this spectral shift was fitted to a sum of three exponentials (Table 2). The red horizontal dotted line corresponds to the band III position in the difference steady-state spectrum.

Table 1. Parameters of Fitted Kinetics Intensity for Hemoglobin and Myoglobin[a]

protein	hemoglobin			myoglobin		
spectral region	τ_1 (amplitude)	τ_2 (amplitude)	constant	τ_1 (amplitude)	τ_2 (amplitude)	constant
band III (integrated area)	25 ± 6 ps (0.42)	120 ± 35 ps (0.41)	0.17	40 ± 12 ps (0.59)	included in constant	0.41
band III (at s. w.)[b]	18 ± 3 ps (0.61)	140 ± 30 ps (0.24)	0.15	27.5 ± 5 ps (0.42)	293 ± 30 ps (0.33)	0.25
band Q (at s. w.)[b]	11 ± 3 ps (0.60)	96 ± 30 ps (0.25)	0.15	12 ± 3 ps (0.40)	205 ± 30 ps (0.37)	0.23
band Q (at s. w.)[b]	12 ± 3 ps (0.74)	114 ± 30 ps (0.24)	0.02	14 ± 2 ps (0.45)	204 ± 30 ps (0.37)	0.18
Soret band (SVD)[c]	10.8 ± 1 ps (0.74)	61.3 ± 6 ps (0.22)	0.04	13 ± 1 ps (0.40)	148 ± 10 ps (0.50)	0.10

[a]Only the structural dynamics are indicated in the table, not the excited-states decay contributions (2−4 ps). [b]At a single wavelength. [c]From singular value decomposition.

Information. At all time delays, the area of Voigtian contour of the fitted bands ν_4 and ν_7 was plotted as a function of time.

3. RESULTS

3.1. Transient Band III Absorption. The band III of deoxy-Hb has an absorption coefficient of 350 $M^{-1}\cdot cm^{-1}$ at 758 nm and shifts upon NO binding at 744 nm, but with a much smaller absorption coefficient (Figures 1 and 2A). After photodissociation of NO with a 50 fs pump pulse, band III immediately appears around 777 nm at +1 ps (Figure 2B), being shifted to the red with respect to the deoxy-Hb steady-state value. When time elapses, band III intensity decreases simultaneously to a blue shift of its central position. The band III is superposed to Q-band, and its evolution must be compared with that of Q-band alone. We thus fitted the absorption kinetics within the band III at a single wavelength (765 nm) and compared with the kinetics fitted at 705 and 785 nm, to probe only the Q-band on each side of band III (Figure

dx.doi.org/10.1021/jp300849y | J. Phys. Chem. B 2012, 116, 4106−4114

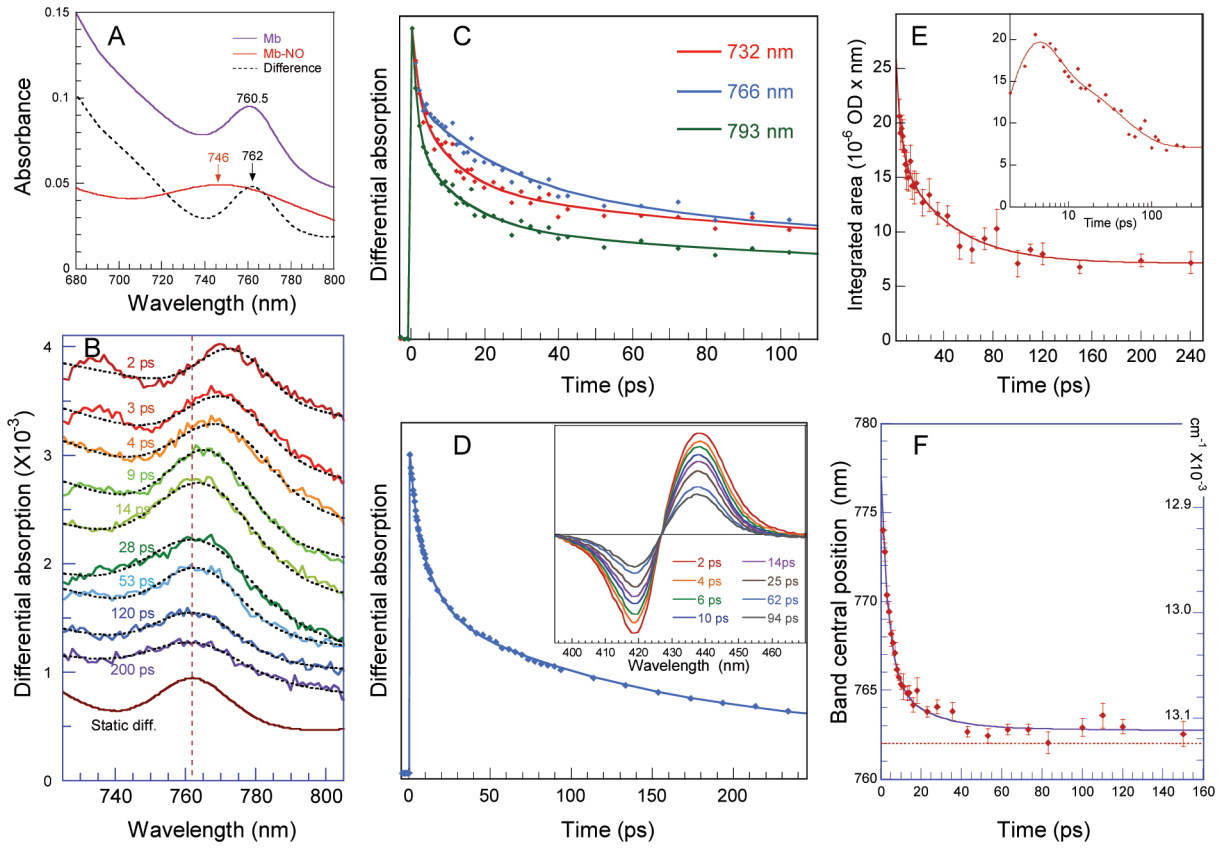

Figure 3. Transient absorption measurement of Mb−NO. (A) Steady-state absorption spectrum in the region of band III for Mb and Mb−NO. (B) Transient difference spectra of band III after NO dissociation. The spectra were not offset and are presented as experimentally obtained. For each spectrum, the black dotted line is a fit of the transient band III to a Gaussian function. The red vertical dotted line corresponds to the position of the band III in the difference steady-state spectrum (brown) scaled for comparison. (C) Kinetics at three single wavelengths after Mb−NO photodissociation. (D) Kinetics of NO rebinding to Mb from global analysis in the Soret band region whose transient spectra are disclosed in the inset. (E) Integrated intensity of band III as a function of time. Each individual transient spectrum was fitted to the sum of a Gaussian function (band III) and an exponential function (tail of the Q-band). The area of the Gaussian represents the integrated intensity of band III. This intensity as a function of time was then fitted to a sum of exponential functions (τ_{ex} = 1.8 ± 0.6 ps; τ_{vib} = 2.5 ± 1 ps; τ_1 = 40 ± 12 ps). Inset: the kinetics on a logarithmic time scale shows the rising absorption of early time spectra (1−4 ps). (F) Central position of the fitted Gaussian as a function of time. The kinetics of this spectral shift was fitted to a sum of three exponentials (Table 2). The red horizontal dotted line corresponds to the band III position in the difference steady-state spectrum.

2C and Table 1). Subsequently, we used the following notation for time constants: τ_{ex} for electronic excited-states decay, τ_{vib} for vibrational relaxation, τ_1 and τ_2 for geminate rebinding phases in Soret and band III intensity kinetics; τ'_{ex}, τ'_1, and τ'_2 are the same time constants but in band III spectral shift kinetics.

Remarkably, the induced absorption decreases more slowly for band III than for the Q-band in the range of 5−50 ps (Figure 2C). We thus recorded the transient absorption of the Soret band in order to follow the NO recombination to Hb (Figure 2D); in this latter case, the high signal/noise ratio allowed us to perform a global analysis of the evolution of the entire band. For fitting all the kinetics (Table 1), a multiexponential function was used, incorporating a component taking into account the vibrational relaxation (τ_{vib} = 3−4 ps) as already observed.[24,26,27] The main component of band III intensity decays with a time constant which is different (τ_1 = 18 ps) from that of Soret band absorption (τ_1 = 10.8 ps), whereas the Q-band decay time constant (τ_1 = 11.5 ps) is similar to that of Soret band intensity decay.

When fitting at a single wavelength, both band III and Q-band contribute to the intensity kinetics, and because band III experiences at the same time a shift of maximum wavelength and an intensity decrease, the real contribution from band III may be slightly distorted. For this reason, we have also fitted the integrated intensity of band III as a function of time (Figure 2E). The integrated intensity was obtained as the area of a Gaussian function. Each individual transient absorption spectrum was fitted to the sum of an exponential function for modeling the tail of the Q-band and a Gaussian function for modeling the band III (inset in Figure 2E).

The kinetics of integrated intensity was fitted to the sum of three exponential components. The first one (τ_{vib} = 2.4 ± 0.3 ps) was readily attributed to vibrational relaxation of the heme in the electronic ground state[24,26,27] and not to conformational relaxation, because the photoexcitation of ferrous Hb in the absence of NO produces a similar ultrafast absorption decay (τ_{vib} = 2.8 ps; Supporting Information Figure S1). The second component of band III integrated intensity kinetics has a time constant (τ_1 = 25 ± 6 ps) larger than that of NO geminate rebinding measured with Soret absorption kinetics (τ_1 = 10.8 ± 1 ps; Table 1) and thus comprises a transition in addition to NO rebinding, which cannot be explained by vibrational relaxation. The longer time constant (τ_2 = 120 ± 35 ps) is assigned to NO geminate rebinding.

dx.doi.org/10.1021/jp300849y | J. Phys. Chem. B 2012, 116, 4106−4114

In the case of Mb−NO, it must be noted that band III also exists for the 6c-NO heme, shifted to 746 nm (Figure 3A), even if the absorption coefficient is smaller than that of deoxy-Mb, contrary to the case of Mb−CO whose band III vanishes (Supporting Information Figure S2). For Mb−NO, we observed a kinetic behavior similar to that of Hb−NO (Figure 3 and Table 1) even more pronounced. The band III intensity decay kinetics (τ_1 = 27.5 ± 5 ps at single wavelength and 40 ± 12 ps for integrated intensity) is different from that in Soret (τ_1 = 13 ps) and Q-band absorption (τ_1 = 14 ps) and is also similar to the Raman band $\nu_{(Fe-His)}$ intensity kinetics (τ_D = 30 ps) as previously reported.[15] The difference in kinetics is clearly seen between 5 and 60 ps in Figure 3C. The fact that band III intensity decreases more slowly than that of the Q-band is illustrated in Supporting Information Figure S3, where the Q-band is normalized at different time delays.

The integrated intensity kinetics of Mb reveal a fast rise (τ_{ex} = 1.8 ± 0.6 ps; Figure 3E inset) that we assign to the decay of electronic excited state, indicating that band III is absent in this electronic excited state, as observed for unliganded Mb (Supporting Information Figure S1b and ref 28.). This rise was not observed in the case of Hb, likely because this decay is faster for Hb.[28]

Despite the quick decrease of band III intensity due to NO rebinding (the absorption coefficient is extremely small for 6c-NO planar heme), the spectral shift is conspicuous. We thus analyzed the evolution of the spectral shift of band III during NO rebinding to both Hb and Mb (Figures 2F and 3F). The central position of the Gaussian contour of band III as a function of time, representing the spectral shift, was fitted to the sum of three exponentials and a constant (Table 2). The

Table 2. Time Constants and Amplitudes of Band III Spectral Shift Components

protein	τ_{vib}	τ'_1	τ'_2
hemoglobin	5.2 ± 2 ps	10.5 ± 2 ps	600 ± 250 ps
	15.2 ± 5 nm	3.1 ± 2 nm	1.8 ± 1 nm
	256 cm^{-1}	53 cm^{-1}	32 cm^{-1}
myoglobin	3.6 ± 1 ps	17 ± 4 ps	800 ± 250 ps
	10.9 ± 2 nm	3.2 ± 2 nm	0.7 ± 0.5 nm
	181 cm^{-1}	56 cm^{-1}	9 cm^{-1}

component with larger contribution (3.6 ps for Mb and 5.2 ps for Hb) is similar to that observed by probing the band III absorption of photodissociated Mb−CO,[21] but also by probing Soret absorption of unliganded photoexcited Mb[26] or anti-Stokes heme in-plane modes.[29,30] This component is thus assigned to excited vibrational states decay, already in the electronic ground state.

Two important observations emerge from these measurements: (i) For both Hb and Mb, there is a component of band III spectral shift with a time constant (τ'_1 = 10.5 ps for Hb and 17 ps for Mb) similar to that obtained from the Soret absorption kinetics for fast NO geminate rebinding (τ_1 = 10.8 and 13 ps, respectively), but different from the band III integrated intensity decay. (ii) Although the shift of band III due to the vibrational excited-states decay has different amplitude for Mb and Hb (181 and 256 cm^{-1}), the subsequent and smaller second component of shift appears similar for Hb (53 cm^{-1}) and Mb (56 cm^{-1}). Within our time range, the third time constant of the shift (τ'_2 = 600−800 ps), whose amplitude is smaller than that of other components, is badly defined and will not be discussed. The total amplitude of the band III spectral shift, including thermal relaxation, is 246 cm^{-1} for Mb but larger for Hb, 341 cm^{-1}. The difference in energy shift for both Hb and Mb is mainly due to thermal relaxation rather than to structural relaxation.

3.2. Time-Resolved Resonance Raman Spectroscopy. We recorded the entire TR[3] spectrum of Hb after NO photodissociation at time delays between +2 and +50 ps (Figure 4) with the purpose of comparing the integrated

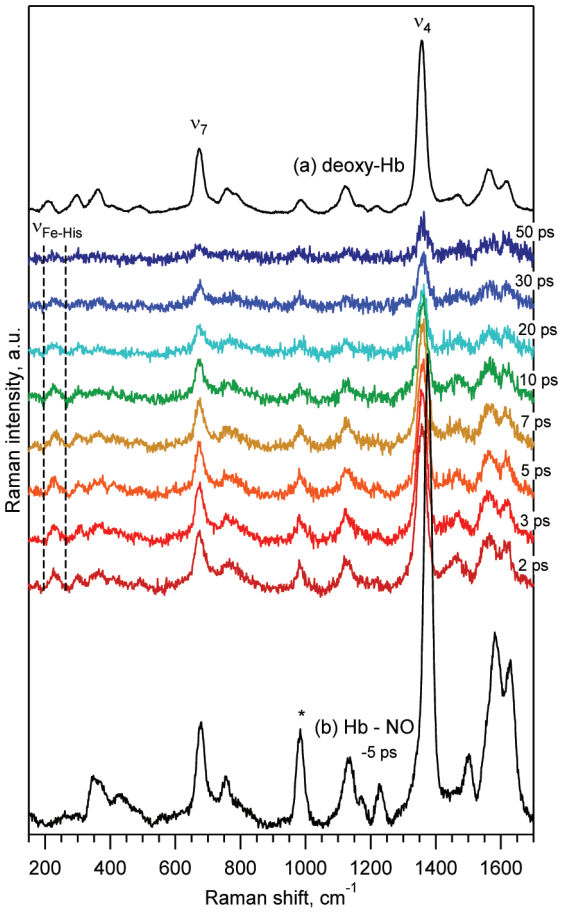

Figure 4. TR3 spectra of Hb from 2 to 50 ps after NO photodissociation: (a) steady-state Raman spectrum of deoxy-Hb recorded with the probe pulse only; (b) Raman spectrum before dissociation of Hb−NO (−5 ps) in the presence of the pump pulse. The vertical dotted lines represent the area for calculating the $\nu_{(Fe-His)}$ integrated intensity whose evolution is reported in Figure 5. The asterisk indicates the band from SO_4^{2-} used to normalize the intensity. The assignment of the modes is given in Supporting Information Table S1. The fitted parameters (Supporting Information Table S2) and fitting of spectra at +2 and +50 ps to a sum of Voigtian functions can be found in the Supporting Information.

intensity decay of the three major Raman bands: the Fe−His stretching mode $\nu_{(Fe-His)}$ and the two major porphyrin in-plane modes ν_4 and ν_7. Importantly, the displayed transient spectra are those of the photoproduct only so that the intensity of all modes decreases as NO rebinds to Hb. Due to its six-coordinate heme, the spectrum of steady-state planar Hb−NO (−5 ps) does not disclose a Fe−His stretching mode, but this mode appears immediately after NO photodissociation (spectrum at +2 ps) and is located at 229 cm^{-1}, being shifted with respect to the deoxy-Hb steady-state value (210 cm^{-1}). At

dx.doi.org/10.1021/jp300849y | J. Phys. Chem. B 2012, 116, 4106−4114

+2 ps, the modes ν_4 and ν_7 are shifted by 22 and 2 cm^{-1} with respect to their values in Hb−NO (−5 ps).

We compared the evolution of the integrated intensity of the modes $\nu_{(Fe-His)}$, ν_4, and ν_7 (Figure 5) with population kinetics

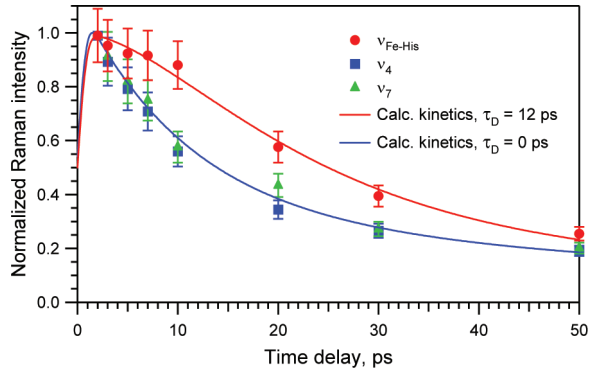

Figure 5. Normalized intensity kinetics. The integrated intensity kinetics of the mode $\nu_{(Fe-His)}$ (red circles) is compared to those of ν_4 (blue squares) and ν_7 (green triangles) for Hb after NO photodissociation. The red curve is calculated according to the rate equations with τ_D = 12 ps, and the blue curve is calculated with τ_D = 0 ps (see details of the model in the Supporting Information, Figure S4). We emphasize that τ_D is not the time constant of the plotted decays but represents the supplementary transition of the iron motion back to the heme plane.

calculated according to the model in Supporting Information Figure S4. This model includes a transition from 6c-domed heme to 6c-planar heme,[15,31] corresponding to the movement of the iron from out-of-heme-plane to in-plane position, triggered by NO binding and whose time constant is τ_D. This population kinetics were calculated in two cases: with the time constant τ_D = 0 ps (which reduces to Soret kinetics), corresponding to an immediate motion of the iron toward its in-plane position, and with τ_D = 12 ps, corresponding to a retarded motion of the iron. The integrated intensity kinetics of the in-plane modes ν_4 and ν_7, which are not sensitive to the position of iron with respect to the heme plane, are identical and follow the calculated kinetics with time constant τ_D = 0 ps, that is to say without contribution of the heme iron motion. Remarkably, the integrated intensity of ν_4 and ν_7 follow the same kinetics as the Soret transient absorption upon NO rebinding. Contrastingly, the integrated intensity of the mode $\nu_{(Fe-His)}$ is different from ν_4 and ν_7 and follows a calculated kinetics incorporating the supplementary transition with time constant τ_D = 12 ps, which represents the subsequent movement of the iron toward the heme plane. This assignment is further discussed below.

4. DISCUSSION

4.1. Origin of Retarded Kinetics. We will now consider possible alternatives for the origin of the retarded kinetics and discuss the consequences of these observations. The kinetic parameters obtained from transient absorption at the Soret and band III and from the $\nu_{(Fe-His)}$ Raman intensity kinetics are summarized in Table 3. We emphasize that τ_D is not an extra exponential component but was obtained as a rate constant from the model in which the iron motion from out-of-plane to in-plane position six-coordinate NO−heme is retarded (Supporting Information Figure S4). Because we compare the time constants during NO rebinding to Mb and Hb for three

Table 3. Comparison of Time Constants Obtained from Transient Absorption Measurements at the Soret Band and Band III and from Raman Intensity Kinetics[a]

protein	hemoglobin (ps)	myoglobin (ps)
NO rebinding from Soret	10.8 ± 1	13 ± 1
band III shift	10.5 ± 2	17 ± 4
band III integrated intensity	25 ± 6	40 ± 12
iron motion τ_D from TR^3	12 ± 6	30 ± 10[a]

[a]Ref 15.

different spectroscopic observables (Soret band, band III, and $\nu_{(Fe-His)}$ Raman mode), we will discuss the possible influence on these kinetics of relaxations previously reported.[21,30,32] Heme cooling and protein relaxation can be probed by TR^3. It was shown that the intensity of ν_4, ν_7, and $\nu_{(Fe-His)}$ Stokes modes is not sensitive to heme cooling following CO photodissociation from Mb, but only the intensity of the anti-Stokes modes is sensitive to cooling.[30,32] We therefore discard heme cooling as the cause of retarded kinetics.

The immediate appearance of both band III and $\nu_{(Fe-His)}$ mode after photodissociation attests to the motion of the iron out of the heme plane, within the instrument response function (0.7 ps for TR^3 and 50 fs for TA). Mizutani and Kitagawa[32] observed an immediate rise of the $\nu_{(Fe-His)}$ intensity due to heme doming after CO dissociation, like after NO dissociation (Figure 4) representing 92% of the signal. It was followed by a 6.5 ps rise, affecting 8% of the $\nu_{(Fe-His)}$ mode intensity assigned to protein relaxation, which can definitively not account for the ∼20% difference in $\nu_{(Fe-His)}$ intensity increase with respect to the Soret, ν_4, and ν_7 kinetics (that we observed for Mb−NO in the time range of 20−40 ps[15]). For Hb−NO (to which NO rebinds faster than to Mb) we observed also a ∼20% difference in normalized intensity between Soret and $\nu_{(Fe-His)}$ in the time range of 10−30 ps. Furthermore, it was unequivocally proven[32] that the minor 8% increase of $\nu_{(Fe-His)}$ intensity in 6.5 ps after CO photodissociation from Mb is not due to global structural changes of the protein because it was also observed for Fe(II)−porphyrin−CO complex, in absence of protein environment. Therefore, the relaxation of the protein which is induced by ligand photodissociation does not affect the retarded intensity of the $\nu_{(Fe-His)}$ mode with respect to ν_4 and ν_7 modes.

If one assumes that only the relaxation due to conformational changes (whatever they are) within the photodissociated 5c-heme in 3.5[21] or 6.5 ps[32] is responsible for the retarded $\nu_{(Fe-His)}$ intensity kinetics, then the $\nu_{(Fe-His)}$ intensity should follow the NO rebinding kinetics once the relaxation is completed, after about 15 ps (2 or 3 times the relaxation constant). However, this is not the case: for Mb, the $\nu_{(Fe-His)}$ kinetics is clearly different from both TA[15] and TA-IR[33] kinetics in the time range of 50−100 ps. To quantitatively investigate the alternative explanation that a heme conformational relaxation in the picosecond time range, induced by NO photodissociation, was at the origin of the difference between Soret and $\nu_{(Fe-His)}$ kinetics, we performed calculations with two different hypotheses. First, considering a protein relaxation induced by NO dissociation from Mb and extended during NO geminate rebinding (model 1 in the Supporting Information), with a time constant of 4.5 ps (initial conditions from dynamic simulation on Mb[34]) or 30 ps (a limit value, equal to that obtained from our Raman data[15]); second, considering a model[15] which includes a nonplanar 6c-NO intermediate with a 30 ps time constant for the iron motion toward the heme plane

dx.doi.org/10.1021/jp300849y | J. Phys. Chem. B 2012, 116, 4106−4114

(model 2 in the Supporting Information). The details of the calculations are described in the Supporting Information, and the result is displayed as calculated kinetics of population species (Supporting Information Figures S5 and S6). From the comparison of kinetics calculated with these different hypotheses, only the model incorporating nonplanar 6c-NO intermediate with a 30 ps time constant can reproduce the kinetics of $\nu_{(Fe-His)}$ integrated intensity. Thus, a transition triggered by NO dissociation (i.e., structural relaxation) cannot explain the observed kinetics, whereas a transition triggered by NO binding does explain the retardation of the kinetics. Similarly, we performed these calculations in the case of Hb−NO, and it appears also evident that only the hypothesis of a nonplanar 6c-NO intermediate with a 12 ps time constant reproduces the experimental results, not the hypothesis of protein relaxation induced by NO dissociation with a 12 ps time constant (Supporting Information Figure S6).

4.2. Origin of the Band III Shift. Previous measurements of the band III intensity were performed[21−23] for unliganded Mb and Mb−CO for which the photodissociated CO does not rebind on the picosecond time scale. Lim et al.[21] found a 3.5 ps component in the band shift position after CO dissociation, and they assigned it to conformational relaxation probed through the iron position. However, they measured also a similar constant in absence of CO (3.4 ps) and assigned it to electronic excited-state decay.[28] After NO dissociation from Mb, we observed same time constant (3.6 ps) that we have assigned to vibrational and not electronic relaxation because band III is absent from the electronic excited-state spectrum (Supporting Information Figure S1 and ref 28.).

We observed that band III intensity and band III position do not behave in the same manner. Band III position was used as a marker of the iron out-of-plane position after CO dissociation from Mb.[21] Since then, the intensities of both band III and the $\nu_{(Fe-His)}$ modes have been theoretically shown to depend upon the distance between the Fe^{2+} and the heme plane.[16−18] Remarkably, we found that both the kinetics of the band III and the transition from domed to planar six-coordinate heme during NO rebinding calculated from the intensity decay of the $\nu_{(Fe-His)}$ mode have time constants larger than NO geminate rebinding (Table 3). Furthermore, both band III and $\nu_{(Fe-His)}$ kinetics have a different time constant compared to Soret and Q-band, but contrastingly the heme in-plane modes ν_4 and ν_7, both sensitive to Fe^{2+} coordination, have the same time constant as Soret kinetics (Figure 5). We thus infer that the band III intensity is a marker of iron out-of-plane displacement with respect to the macrocycle plane, a fact that could not be established from previous TA measurements involving CO photodissociation, and exactly as predicted from theory by Stavrov.[17]

4.3. Relation with Heme Protein Allostery. We have assigned the origin of delayed (τ_D) in-plane iron motion to structural constraints exerted by the protein structure on the heme.[15] Tensions in the T-state of Hb have been remarkably demonstrated[35] to be responsible for large atomic motions and are exerted on the Fe−His bond so that it breaks when CN^- is liganded to the heme in the crystal structure.[35] Therefore, due to the presence of such tensions, an immediate iron motion upon diatomic binding is very unlikely. This implies that, after NO dissociation, the heme environment immediately starts to move toward the T-state configuration (not the entire protein, which reacts in the ∼0.1−1 μs time range[9,11,12]). We remind here that, after diatomic ligand detachment, the iron moves out of the heme plane instantaneously, in contrast to the reverse binding reaction that we observe here. Thus, a structural relaxation in the heme pocket or its close vicinity has taken place faster than τ_D, as a response to immediate out-of-plane motion of the heme iron toward proximal side chain. Indeed, time-resolved circular dichroism studies reported a motion of the proximal histidine with 7 ps time constant after CO dissociation from Mb[36] and Hb[37] and a TR^3 study, probing the aromatic Mb side chains in the heme vicinity, observed localized structural motions with 8 ps time constant.[38] Therefore, this relaxation starts before NO rebinding, rationalizing the existence of constraints due to the protein structure exerted on the proximal histidine. Furthermore, constraints that retard the iron motion back to the heme plane can also exist before ligand dissociation, in the six-coordinate state. These constraints (and thus τ_D) depend upon the nature of the heme protein.[15] In the case of tetrameric Hb, simultaneous photodissociation of NO from all four subunits cannot be realized since the pump pulse intensity is not saturating. Thus, the interactions exerted by the still-liganded subunits on the dissociated one possibly influence τ_D which could be different if the four Hb subunits were simultaneously dissociated.

As for the position of band III, it must be noted that, so far, it was investigated only for Mb after CO photolysis,[21,22] probing relaxation of the dissociated heme, whereas we probed here the band III during NO rebinding, so that the only common process is the excited-states relaxation. Apart from this latter process, we observed that band III shifts with a time constant similar to that of the Soret band kinetics due to NO rebinding, but different from the band III intensity decrease, that we correlated to retarded in-plane iron motion originally discovered from TR^3 measurements. Since the band III corresponds to a charge-transfer transition, it depends on the Fe^{2+} spin state and on the d_{yz} orbital energy,[19] but also on other factors such as vibronic interactions or electric field exerted on the heme,[17,18] so that its position (energy of the transition) depends on the iron coordination state.[19] This can explain the presence of a component in spectral shift kinetics similar to Soret kinetics during NO rebinding, suggesting that band III shift is less influenced by the iron position, contrary to its intensity.

We have observed a complex spectral shift of band III after NO dissociation. The amplitude of the spectral shift due to vibrational relaxation (τ_{ex} = 3.6−5.2 ps) is much larger for Hb than for Mb (256 and 181 cm^{-1}), suggesting different amplitudes of heme cooling and different constraints in the heme pocket between both proteins. However, the spectral shift associated with NO rebinding to Hb (53 cm^{-1}) and to Mb (56 cm^{-1}) is the same. Given that band III is a charge-transfer transition from π porphyrin orbitals to d iron orbitals,[19,20] a larger change of the transition energy in Hb than in monomeric Mb would reflect a different geometric change induced by NO release, influencing the molecular orbitals through a change in local electric field.[17,39,40] In this line, it was shown that band III position depends upon the substates after CO dissociation and is also sensitive to the nature of the distal side chains.[41] This dependence must also apply after NO dissociation and should be the origin of the long component of band III shift. As noted by Christian et al.[42] "there is no direct and simple correlation between $\nu_{(Fe-His)}$ and band III position", which may depend on the distal environment as well as on heme constraints which influence orbital energies.

After the shift due to NO rebinding, band III did not completely reach its steady-state value for Hb and Mb so that the heme of both proteins did not yet relax to its unliganded conformation at delay +100 ps after NO dissociation. This difference is again larger for Hb than for Mb. Remarkably, a difference of shift between both proteins was also measured at +10 ns after CO dissociation, 10 nm for Hb, but no shift for Mb.[43] Whatever its nature, a more important structural change occurs in the heme vicinity upon NO release from Hb than from Mb, which could be correlated with larger structural constraints in the heme pocket of tetrameric Hb involved in allosteric transitions.

In conclusion, the band III integrated intensity kinetics is retarded with respect to that of NO geminate rebinding measured in Soret and Q-bands kinetics. Similarly, the intensity decay of $\nu_{(Fe-His)}$ mode in TR^3 measurements is retarded with respect to the ν_4 and ν_7 modes and to Soret absorption transient absorption kinetics. These observations are rationalized by the existence of a transient heme species having six-coordinate out-of-plane iron immediately after NO rebinding and agree with theoretical work which hypothesized that $\nu_{(Fe-His)}$ stretching and band III intensities depend upon the position of iron with respect to the heme plane. Thus, the iron motion toward a planar 6c-NO heme does not occur immediately, but with a constant of 30 ps for Mb and 12 ps for Hb (Figure 6).

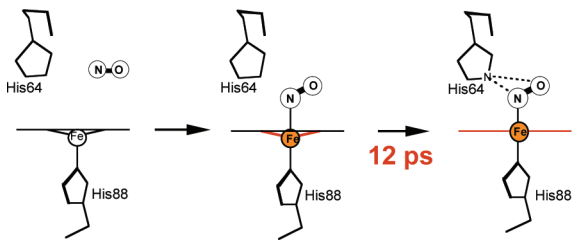

Figure 6. Model summarizing the dynamics of the heme iron upon nitric oxide binding to hemoglobin.

■ ASSOCIATED CONTENT

Supporting Information

Transient absorption spectra, kinetic models and calculations, table of Raman bands assignments, table of fitted parameters of Raman bands, fitting of the Raman spectra at +2 and +50 ps. This material is available free of charge via the Internet at http://pubs.acs.org.

■ AUTHOR INFORMATION

Corresponding Author

*E-mail: michel.negrerie@polytechnique.fr. Phone: 133 69 33 50 52. Fax: 133 69 33 50 84.

Notes

The authors declare no competing financial interest.

■ ACKNOWLEDGMENTS

We thank Fondation pour la Recherche Médicale for supporting our work with a Ph.D. fellowship attributed to B.-K.Y.

■ ABBREVIATIONS

TA, transient absorption; TR^3, time-resolved resonance Raman spectroscopy; TA-IR, transient absorption in infrared; Hb, hemoglobin; Mb, myoglobin; 5c-, 6c-heme, five-, six-coordinate heme

■ REFERENCES

(1) Perutz, M. F. *Nature* **1970**, *228*, 726−793.
(2) Perutz, M. F.; Wilkinson, A. J.; Paoli, M.; Dodson, G. G. *Annu. Rev. Biophys. Biomol. Struct.* **1998**, *27*, 1−34.
(3) Monod, J.; Wyman, J.; Changeux, J. P. *J. Mol. Biol.* **1965**, *12*, 88−118.
(4) Hofrichter, J.; Sommer, J. H.; Henry, E. R.; Eaton, W. A. *Proc. Natl. Acad. Sci. U.S.A.* **1983**, *80*, 2235−2239.
(5) Findsen, E. W.; Friedman, J. M.; Ondrias, M. R.; Simon, S. R. *Science* **1985**, *229*, 661−665.
(6) Friedman, J. M. *Science* **1985**, *228*, 1273−1280.
(7) Petrich, J. W.; Lambry, J. C.; Kuczera, K.; Karplus, M.; Poyart, C.; Martin, J. L. *Biochemistry* **1991**, *30*, 3975−3987.
(8) Rodgers, K. R.; Spiro, T. G. *Science* **1994**, *265*, 1697−1699.
(9) Jayaraman, V.; Rodgers, K. R.; Mukkerji, I.; Spiro, T. G. *Science* **1995**, *269*, 1843−1848.
(10) Jayaraman, V.; Spiro, T. G. *Biospectroscopy* **1996**, *2*, 311−316.
(11) Yamaoka, M.; Sugishima, M.; Noguchi, M.; Fukuyama, K.; Mizutani, Y. *J. Raman Spectrosc.* **2011**, *42*, 910−916.
(12) Knapp, J. E.; Pahl, R.; Srajer, V.; Royer, W. E. *Proc. Natl. Acad. Sci. U.S.A.* **2006**, *103*, 7649−7654.
(13) Martin, J. L.; Migus, A.; Poyart, C.; Astier, R.; Antonetti, A. *EMBO J.* **1983**, *2*, 1815−1819.
(14) Franzen, S.; Lambry, J. C.; Bohn, B.; Poyart, C.; Martin, J. L. *Nat. Struct. Biol.* **1994**, *1*, 230−233.
(15) Kruglik, S. G.; Yoo, B.-K.; Franzen, S.; Vos, M. H.; Martin, J.-L.; Negrerie, M. *Proc. Natl. Acad. Sci. U.S.A.* **2010**, *107*, 13678−13683.
(16) Stavrov, S. S. *Biophys. J.* **1993**, *6*, 1942−1950.
(17) Stavrov, S. S. *Chem. Phys.* **2001**, *271*, 145−154.
(18) Stavrov, S. S. *Biopolymers* **2004**, *74*, 37−40.
(19) Eaton, W. A.; Hanson, L. K.; Stephens, P. J.; Sutherland, J. C.; Dunn, J. B. R. *J. Am. Chem. Soc.* **1978**, *100*, 4991−5003.
(20) Sage, J. T.; Morikis, D.; Champion, P. M. *Biochemistry* **1991**, *30*, 1227−1237.
(21) Lim, M. H.; Jackson, T. A.; Anfinrud, P. A. *Proc. Natl. Acad. Sci. U.S.A.* **1993**, *90*, 5801−5804.
(22) Jackson, T. A.; Lim, M. H.; Anfinrud, P. A. *Chem. Phys.* **1994**, *180*, 131−140.
(23) Huang, J.; Leone, M.; Boffi, A.; Friedman, J. M.; Chiancone, E. *Biophys. J.* **1996**, *70*, 2924−2929.
(24) Negrerie, M.; Cianetti, S.; Vos, M. H.; Martin, J. L.; Kruglik, S. G. *J. Phys. Chem. B* **2006**, *110*, 12766−12781.
(25) Kruglik, S. G.; Lambry, J.-C.; Martin, J.-L.; Vos, M. H.; Negrerie, M. *J. Raman Spectrosc.* **2011**, *42*, 265−275.
(26) Petrich, J. W.; Poyart, C.; Martin, J. L. *Biochemistry* **1988**, *27*, 4049−4060.
(27) Li, P.; Sage, J. T.; Champion, P. M. *J. Chem. Phys.* **1992**, *97*, 3214−3227.
(28) Lim, M. H.; Jackson, T. A.; Anfinrud, P. A. *J. Phys. Chem.* **1996**, *100*, 12043−12051.
(29) Lingle, R.; Xu, X.; Zhu, H.; Yu, S. C.; Hopkins, J. B. *J. Phys. Chem.* **1991**, *95*, 9320−9331.
(30) Mizutani, Y.; Kitagawa, T. *Science* **1997**, *278*, 443−446.
(31) Ionascu, D.; Gruia, F.; Ye, X.; Yu, A. C.; Rosca, F.; Beck, C.; Demidov, A.; Olson, J. S.; Champion, P. M. *J. Am. Chem. Soc.* **2005**, *127*, 16921−16934.
(32) Mizutani, Y.; Kitagawa, T. *J. Phys. Chem. B* **2001**, *105*, 10992−10999.
(33) Kim, S.; Jin, G.; Lim, M. *J. Phys. Chem. B* **2004**, *108*, 20366−20375.
(34) Kuczera, K.; Lambry, J. C.; Martin, J.-L.; Karplus, M. *Proc. Natl. Acad. Sci. U.S.A.* **1993**, *90*, 5805−5807.

(35) Paoli, M.; Dodson, G.; Liddington, R. C.; Wilkinson, A. J. *J. Mol. Biol.* **1997**, *271*, 161−167.
(36) Dartigalongue, T.; Hache, F. *Chem. Phys. Lett.* **2005**, *415*, 313−316.
(37) Dartigalongue, T. Conformational dynamics of myoglobin studied by time-resolved circular dichroism. Ph.D. Thesis Dissertation, Ecole Polytechnique, Palaiseau, France, 2005.
(38) Sato, A.; Gao, Y.; Kitagawa, T.; Mizutani, Y. *Proc. Natl. Acad. Sci. U.S.A.* **2007**, *104*, 9627−9632.
(39) Franzen, S.; Wallace-Williams, S. E.; Shreve, A. P. *J. Am. Chem. Soc.* **2002**, *124*, 7146−7155.
(40) Franzen, S.; Moore, L. J.; Woodruff, W. H.; Boxer, S. G. *J. Phys. Chem. B* **1999**, *103*, 3070−3072.
(41) Nienhaus, K.; Lamb, D. C.; Deng, P.; Nienhaus, U. *Biophys. J.* **2002**, *82*, 1059−1067.
(42) Christian, J. F.; Unno, M.; Sage, J. T.; Champion, P. M.; Chien, E.; Sligar, S. G. *Biochemistry* **1997**, *36*, 11198−11204.
(43) Sassaroli, M.; Rousseau, D. L. *Biochemistry* **1987**, *26*, 3092−3098.